

55. Neoplasia II

A wide variety of other neoplasias may affect the head and neck. In the parapharyngeal space, these include neural tumors, salivary gland tumors, and paragangliomas. Glomus jugulare (Fig. 55.1) and carotid body (glomus) paragangliomas are distinguished by their location, the former arising from the jugular fossa and the latter at the carotid bifurcation. Glomus vagale tumors also occur. All tend to demonstrate a characteristic salt (less common) and pepper (more common) pattern on unenhanced MR. The salt or high SI areas within a tumor correspond to subacute hemorrhage or flow – which can be slow or fast, the latter giving rise to high signal intensity on a short TE GRE scan (Fig. 55.1A). The pepper or low SI areas correspond to high-velocity arterial flow voids (typically seen on FSE scans). Note the internal carotid artery (with high SI due to the use of a short TE GRE scan) along the anterior margin of the lesion. This highly vascular tumor also demonstrates intense enhancement (black arrow) on CE T1WI (Fig. 55.1B). Intraluminal extension into the internal jugular vein can occur.



Fig. 55.1

The parotid gland is the most common location for salivary gland tumors, with pleomorphic adenomas being the most common tumor in the parotid. Most pleomorphic adenomas are

sharply marginated, low SI on T1WI - well seen against the high SI of the normal, fatty parotid, and high SI on T2WI. Differentiation from a cystic lesion is easy, as these lesions tend to enhance brightly and uniformly. Malignant entities (i.e. mucoepidermoid and adenoid cystic carcinoma) cannot be differentiated with certainty from benign salivary gland tumors on MR. A nonenhancing unilateral parotid lesion is likely a Warthin tumor (with 20% multifocal) – which classically arises in the parotid tail (near the angle of the mandible), while a truly cystic lesion likely represents a brachial cleft malformation. Ocular melanoma is the most common malignant intraocular malignancy in adults, arising from the uveal structures. Paramagnetic effects of melanin (due to metal scavenging) shorten T1 and T2. Thus, ocular melanoma classically appears hyper- and hypointense on T1 and T2WI, respectively, compared to vitreous fluid. Melanoma may be distinguished from surrounding fluid or hemorrhage with CE T1WI, due to moderate, diffuse enhancement. Retinoblastomas may demonstrate similar MR SI characteristics to melanoma. Detection of calcification—which is limited on MR—on CT distinguishes retinoblastoma from melanoma, as does patient age since retinoblastoma is found almost exclusively in children. The presence of trilateral retinoblastoma (bilateral in the orbits and a third pineal or suprasellar lesion) is well-evaluated on MR. The retinoblastoma in Fig. 55.2 A, B demonstrates characteristic low SI appearance on (A) T2WI, and although not shown, was slightly hyperintense on T1WI pre-contrast. Mild enhancement is present on (B) CE FS T1WI. FS images were obtained in this case to suppress the high SI from retrobulbar fat which would otherwise obscure evaluation for optic nerve enhancement, which would be indicative of contiguous tumor spread. Growth of the tumor beneath the retina (subretinal) is described as exophytic spread and can lead to retinal detachment, present in this case and seen as a moderate SI linear structure anterior to the mass in Fig. 55.2 A, B.

Amelanotic melanoma and ocular metastases are different in appearance than melanotic melanoma, with high and low SI on T2 and T1WI, respectively, as seen with most malignancies. Exceptions to this include mucinous and hemorrhagic adenocarcinomas, the former illustrated in Fig. 55.2 C, D. The lesion is best identified by hypointensity on the (C) T2WI (white arrow), with subtle, moderate SI on (D) T1WI. Fluid beneath the retinal detachment also present in this case is best seen as intermediate SI on the (D) T1WI (black arrow). Due to its vascularity, the uvea is the most frequent site of metastatic disease to the orbit.

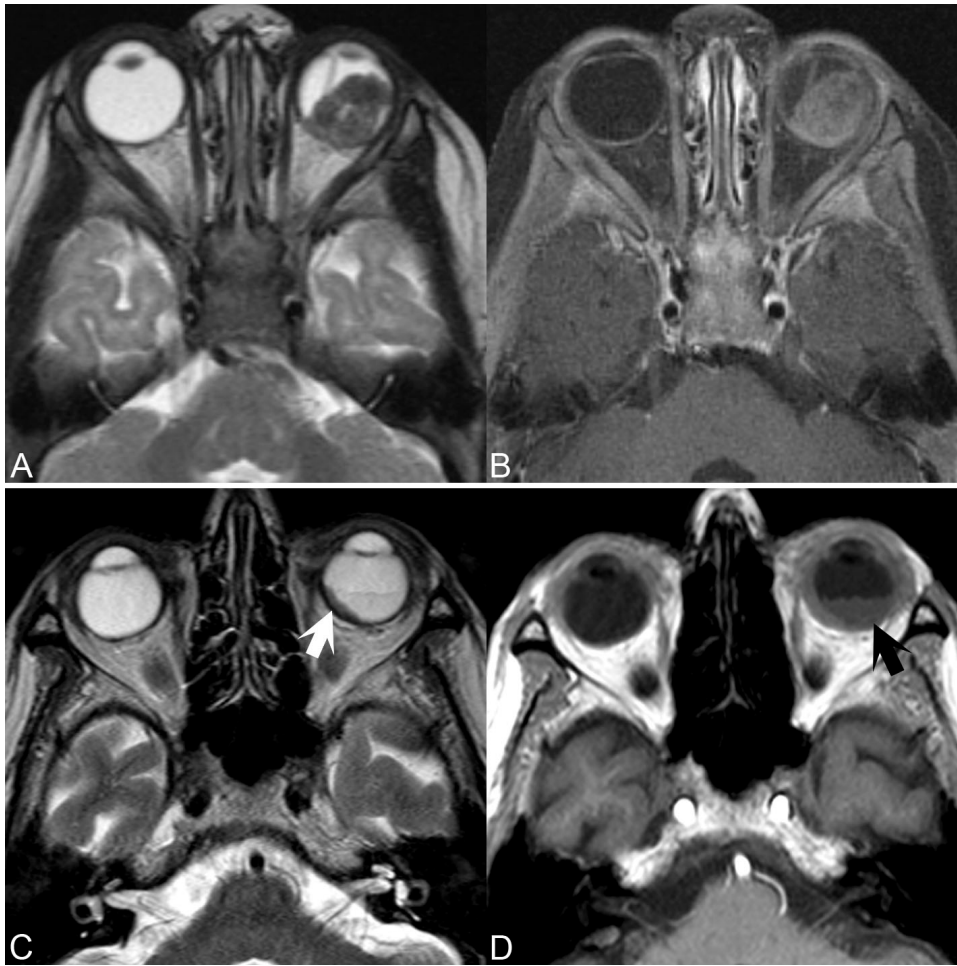


Fig. 55.2